Transition State Structure of the Solvolytic Hydrolysis of NAD^+ †

Paul J. Berti and Vern L. Schramm*

Contribution from the Department of Biochemistry, Albert Einstein College of Medicine, 1300 Morris Park Avenue, Bronx, New York 10461

Received April 25, 1997⊗

Abstract: The transition state structure has been determined for the pH-independent solvolytic hydrolysis of NAD^+. The structure is based on kinetic isotope effects (KIEs) measured for NAD^+'s labeled in various positions of the ribose ring and in the leaving group nitrogen. The KIEs for reactions performed at 100 °C in 50 mM NaOAc (pH 4.0) were as follows: 1-^{15}N, 1.020 ± 0.007; 1′-^{14}C, 1.016 ± 0.002; [1-^{15}N,1′-^{14}C], 1.034 ± 0.002; 1′-^{3}H, 1.194 ± 0.005; 2′-^{3}H, 1.114 ± 0.004; 4′-^{3}H, 0.997 ± 0.001; 5′-^{3}H, 1.000 ± 0.003; 4′-^{18}O, 0.988 ± 0.007. The transition state structure was determined using bond energy/bond order vibrational analysis to predict KIEs for trial transition state models. The structure that most closely matches the experimental KIEs defines the transition state. A structure interpolation method was developed to generate trial transition state structures and thereby systematically search reaction coordinate space. Structures are generated by interpolation between reference structures, reactant NAD^+ and a hypothetical {ribo-oxocarbenium ion plus nicotinamide} structure. The point in reaction coordinate space where all the predicted KIEs matched the measured ones was considered to locate the transition state structure. This occurred when the residual bond order to the leaving group nicotinamide, $n_{LG,TS}$, was 0.02 (bond length = 2.65 Å) and the bond order to the approaching nucleophile, $n_{Nu,TS}$, was 0.005 (3.00 Å). Thus, bond-breaking and bond-making in this A_ND_N reaction are asynchronous, and the transition state has a highly oxocarbenium ion-like character.

Introduction

As the chemical benchmark for studies of the reactions catalyzed by the ADP-ribosylating bacterial toxins, cholera,[1,2] pertussis,[3,4] and diphtheria toxin,[5] the transition state structure for the pH-independent solvolytic hydrolysis of NAD^+ has been determined. Nucleophilic substitutions on glycosides (including hydrolysis) have been studied by a variety of kinetic methods, including the extensive use of kinetic isotope effects[2,4,6−18] (KIEs[19]) to elucidate mechanism. Mechanistic studies have uniformly demonstrated that these reactions proceed through transition states that are on the borderline between A_ND_N and $D_N + A_N$ mechanisms for both nonenzymatic[20−26] and enzymatic[27−34] reactions, as have studies of nonenzymatic[17,18,35−40] and enzymatic NAD^+ hydrolysis.[17,18,35−37,41−43]

Intrinsic KIEs report directly on events at the transition state of the reaction. Specifically, KIEs reflect the change in the vibrational environment of the labeled atom between the reactant and the irreversible transition state(s) of the reaction. A vibrationally less restrained environment, resulting from decreased bond orders or changes in bond angles, will lead to normal KIEs (i.e., the light atom reacts more quickly than the heavy atom, $^{light}k/^{heavy}k > 1$). A vibrationally more restrained

† This work was supported by NIH Research Grant AI34342 and a postdoctoral fellowship from the Natural Sciences and Engineering Research Council (Canada) to P.J.B.

* Corresponding author: phone, (718) 430-2813; fax, (718) 430-8565; e-mail, vern@aecom.yu.edu.

⊗ Abstract published in *Advance ACS Abstracts,* November 15, 1997.

(1) Rising, K. A.; Schramm, V. L. *J. Am. Chem. Soc.* **1994**, *116*, 6531−6536.
(2) Rising, K. A.; Schramm, V. L. *J. Am. Chem. Soc.* **1997**, *119*, 27−37.
(3) Scheuring, J.; Schramm, V. L. *J. Am. Chem. Soc.* **1995**, *117*, 12653−12654.
(4) Scheuring, J.; Schramm, V. L. *Biochemistry* **1997**, *36*, 4526−4534.
(5) Berti, P. J.; Blanke, S. R.; Schramm, V. L. *J. Am. Chem. Soc.* **1997**, *119*, 12079−12088.
(6) Craze, G.-A.; Kirby, A. J.; Osborne, R. *J. Chem. Soc., Perkin Trans. 2* **1978**, 357−368.
(7) Mentch, F.; Parkin, D. W.; Schramm, V. L. *Biochemistry* **1987**, *26*, 921−930.
(8) Withers, S. G.; Jullien, M.; Sinnott, M. L.; Viratelle, O. M.; Yon, J. M. *Eur. J. Biochem.* **1978**, *87*, 249−256.
(9) Burton, J.; Sinnott, M. L. *J. Chem. Soc., Perkin Trans. 2* **1983**, 359−364.
(10) Ashwell, M.; Guo, X.; Sinnott, M. L. *J. Am. Chem. Soc.* **1992**, *114*, 10158−10166.
(11) Bennet, A. J.; Sinnott, M. L. *J. Am. Chem. Soc.* **1986**, *108*, 7287−7294.
(12) Guo, X.; Laver, W. G.; Vimr, E.; Sinnott, M. L. *J. Am. Chem. Soc.* **1994**, *116*, 5572−5578.
(13) Horenstein, B. A.; Bruner, M. *J. Am. Chem. Soc.* **1996**, *118*, 10371−10379.
(14) Goitein, R. K.; Chelsky, D.; Parsons, S. M. *J. Biol. Chem.* **1978**, *253*, 2963−2971.
(15) Horenstein, B. A.; Parkin, D. W.; Estupinan, B.; Schramm, V. L. *Biochemistry* **1991**, *30*, 10788−10795.
(16) Romero, R.; Stein, R.; Bull, H. G.; Cordes, E. H. *J. Am. Chem. Soc.* **1978**, *100*, 7620−7624.
(17) Bull, H. G.; Ferraz, J. P.; Cordes, E. H.; Ribbi, A.; Apitz-Castro, R. *J. Biol. Chem.* **1978**, *253*, 5186−5192.
(18) Ferraz, J. P.; Bull, H. G.; Cordes, E. H. *Arch. Biochem. Biophys.* **1978**, *191*, 431−436.

(19) Abbreviations: CI, confidence interval; EIE, equilibrium isotope effect; KIE, kinetic isotope effect; LFER, linear free energy relationship; NAD^+, nicotinamide adenine dinucleotide; n_{LG} and n_{Nu}, bond orders to the leaving group and to the incipient nucleophile; n_{X-Y}, bond order between atoms X and Y; r_{X-Y}, bond length between atoms X and Y; TS, transition state.

(20) Sinnott, M. L.; Jencks, W. P. *J. Am. Chem. Soc.* **1980**, *102*, 2026−2032.
(21) Kneir, B. L.; Jencks, W. P. *J. Am. Chem. Soc.* **1980**, *102*, 6789−6798.
(22) Amyes, T. L.; Jencks, W. P. *J. Am. Chem. Soc.* **1989**, *111*, 7888−7900.
(23) Banait, N. S.; Jencks, W. P. *J. Am. Chem. Soc.* **1991**, *113*, 7951−7958.
(24) Banait, N. S.; Jencks, W. P. *J. Am. Chem. Soc.* **1991**, *113*, 7958−7963.
(25) Cherian, X. M.; Van Arman, S. A.; Czarnick, A. W. *J. Am. Chem. Soc.* **1990**, *112*, 4490−4498.
(26) Huang, X.; Surry, C.; Hiebert, T.; Bennet, A. J. *J. Am. Chem. Soc.* **1995**, *117*, 10614−10621.
(27) Sinnott, M. L. *Chem. Rev.* **1990**, *90*, 1171−1202.
(28) Padmaperuma, B.; Sinnott, M. L. *Carbohydr. Res.* **1993**, *250*, 79−86.
(29) Legler, G. *Carbohydr. Res.* **1993**, *250*, vii−xx.
(30) Tull, D.; Withers, S. G. *Biochemistry* **1994**, *33*, 6363−6370.

S0002-7863(97)01316-4 CCC: $14.00

environment will lead to inverse KIEs, $^{light}k/^{heavy}k < 1$. A family of KIEs for substrates labeled at different positions provides sufficient information to make specific, quantitative statements about transition state structures.

Transition state structures for nonenzymatic[7,44] and enzymatic[2,5,7,15,45−50] *N*-ribosidic hydrolyses have been determined by analysis of families of KIEs using the bond energy/bond order vibrational analysis method.[51,52] The KIE at each labeled position is predicted from the partition functions of the normal vibrational modes derived from the reactant and the trial transition state structures. The transition state structure is varied until the predicted KIEs match the experimental ones. Analysis of these transition state structures has led to the design and synthesis of potent competitive inhibitors of nucleoside hydrolases, with K_i's to 2 nM.[53−57]

Transition state modeling from bond-vibrational methods has previously been done on an ad hoc basis, that is, geometrical parameters that are expected to affect the KIEs are varied individually in chemically reasonable models of the transition state until the predicted KIEs match the measured ones. In this study, we have developed a method of transition state analysis based on structure interpolation between reference structures. An algorithm is used that predicts the structure of the substrate molecule throughout reaction coordinate space. Trial transition state structures are generated systematically, and the predicted transition state structure is the one that most closely matches the experimental KIEs.

Scheme 1

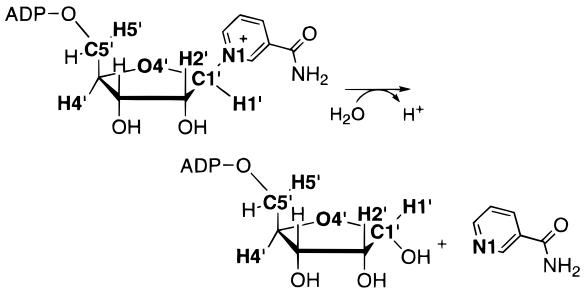

A specific aim of this study was to develop this structure interpolation method of transition state prediction. The quality of the method can be judged on its ability to predict KIEs at each labeled position that match the measured KIEs and to predict a transition state structure in agreement with the literature data on NAD^+ hydrolysis. A robust algorithm should accomplish these goals with a minimum of arbitrary or ad hoc adjustments.

The transition state structure for solvolytic NAD^+ hydrolysis (Scheme 1) has been solved using this approach. Comparison of this transition state structure with those for the enzymatic reactions will show how these enzymes modify the intrinsic reaction energetics of the substrates to lower the transition state energy. These results will also be relevant to other enzymatic ADP-ribosylation reactions such as poly(ADP-ribose)[58] and cyclic ADP-ribose[59] synthases and other ADP-ribosyl transferases.[60]

Experimental Procedures

Synthesis of radiolabeled NAD^+'s[1] and the method of KIE determination by liquid scintillation counting[2] have been described previously. The hydrolytic reactions were carried out at 100 °C in 50 mM NaOAc (pH 4.0). Synthesis of 4′-^{18}O labeled NAD^+ and mass spectrometric measurement of the 4′-^{18}O KIE are described in the following paper.[5] Rates of NAD^+ hydrolysis were determined using [4-^{3}H]NAD^+ as described previously.[2]

Determination of Transition States Using Structure Interpolation

KIE Calculation. The transition state structure of NAD^+ hydrolysis was modeled using the bond energy/bond order vibrational analysis method.[51,52] Given structures of the reactant and transition state of a reaction and appropriately defined force constants for bond stretches, bond angle bends, and bond torsions, the program BEBOVIB[61] predicts the KIE at each isotopically labeled position using the partition function of Bigeleisen and Wolfsberg.[62] The transition state structure is varied until the predicted KIEs match the experimental ones.

"Bond order" is the Pauling bond order

$$n_i = \exp[(r_1 - r_i)/0.3]$$

where r_1 is the bond length of a single bond. Single bond lengths were as follows: C−C, 1.526 Å; C−N, 1.475 Å; C−O, 1.41 Å; C−H, 1.09 Å. These values were used in BEBOVIB

(31) Tanaka, Y.; Tao, W.; Blanchard, J. S.; Hehre, E. J. *J. Biol. Chem.* **1994**, *269*, 32306−32312.
(32) Wang, Q. P.; Graham, R. W.; Trimbur, D.; Warren, R. A. J.; Withers, S. G. *J. Am. Chem. Soc.* **1994**, *116*, 11594−11595.
(33) Braun, C.; Brayer, G. D.; Withers, S. G. *J. Biol. Chem.* **1995**, *270*, 26778−26781.
(34) McIntosh, L. P.; Hand, G.; Johnson, P. E.; Joshi, M. D.; Korner, M.; Plesniak, L. A.; Ziser, L.; Wakarchuk, W. W.; Withers, S. G. *Biochemistry* **1996**, *35*, 9958−9966.
(35) Tarnus, C.; Schuber, F. *Bioorg. Chem.* **1987**, *15*, 31−42.
(36) Oppenheimer, N. J. *Mol. Cell. Biochem.* **1994**, *138*, 245−251.
(37) Handlon, A. L.; Xu, C.; Muller-Steffner, H. M.; Schuber, F.; Oppenheimer, N. J. *J. Am. Chem. Soc.* **1994**, *116*, 12087−12088.
(38) Johnson, R. W.; Marschner, T. M.; Oppenheimer, N. J. *J. Am. Chem. Soc.* **1988**, *110*, 2257−2263.
(39) Oppenheimer, N. J.; Tashma, R. *Biochemistry* **1992**, *31*, 2195.
(40) Handlon, A. L.; Oppenheimer, N. J. *J. Org. Chem.* **1991**, *56*, 5009−5010.
(41) Tarnus, C.; Muller, H. M.; Schuber, F. *Bioorg. Chem.* **1988**, *16*, 38−51.
(42) Schuber, F.; Travo, P.; Pascal, M. *Bioorg. Chem.* **1979**, *8*, 83−90.
(43) Bohmer, J.; Jung, M.; Sehr, P.; Fritz, G.; Popoff, M.; Just, I.; Aktories, K. *Biochemistry* **1996**, *35*, 282−289.
(44) Parkin, D. W.; Leung, H. B.; Schramm, V. L. *J. Biol. Chem.* **1984**, *259*, 9411−9417.
(45) Kline, P. C.; Schramm, V. L. *Biochemistry* **1995**, *34*, 1153−1162.
(46) Scheuring, J.; Berti, P. J.; Schramm, V. L. Submitted for publication.
(47) Kline, P. C.; Schramm, V. L. *Biochemistry* **1993**, *32*, 13212−13219.
(48) Parkin, D. W.; Mentch, F.; Banks, G. A.; Horenstein, B. A.; Schramm, V. L. *Biochemistry* **1991**, *30*, 4586−4594.
(49) Parkin, D. W.; Schramm, V. L. *Biochemistry* **1987**, *26*, 913−920.
(50) Parkin, D. W.; Schramm, V. L. *J. Biol. Chem.* **1984**, *259*, 9418−9425.
(51) Sims, L. B.; Lewis, D. E. In *Isotope effects: Recent developments in theory and experiment*; Buncel, E., Lee, C. C., Eds.; Elsevier: New York, 1984; Vol. 6, pp 161−259.
(52) Johnston, H. S. *Gas-phase reaction rate theory*; Ronald Press: Co.: New York, 1966.
(53) Horenstein, B. A.; Schramm, V. L. *Biochemistry* **1993**, *32*, 9917−9925.
(54) Horenstein, B. A.; Schramm, V. L. *Biochemistry* **1993**, *32*, 7089−7097.
(55) Horenstein, B. A.; Zabinski, R. F.; Schramm, V. L. *Tetrahedron Lett.* **1993**, *34*, 7213−7216.
(56) Boutellier, M.; Horenstein, B. A.; Semenyaka, A.; Schramm, V. L.; Ganem, B. *Biochemistry* **1994**, *33*, 3994−4000.
(57) Deng, H.; Chan, A. W.-Y.; Bagdassarian, C. K.; Estupinan, B.; Ganem, B.; Callender, R. H.; Schramm, V. L. *Biochemistry* **1996**, *35*, 6037−6047.
(58) Sugimura, T.; Miwa, M. *Mol. Cell. Biochem.* **1994**, *138*, 5−12.
(59) Lee, H. C.; Galione, A.; Walseth, T. F. *Vitam. Horm.* **1994**, *48*, 199−257.
(60) Donnelly, L. E.; Boyd, R. S.; Clifford, C. P.; Olmos, G.; Allport, J. R.; Lo, G.; MacDermot, J. *Biochem. Pharm.* **1994**, *48*, 1669−1675.
(61) Sims, L. B.; Burton, G. W.; Lewis, D. E. *BEBOVIB-IV, QCPE No. 337*; Quantum Chemistry Program Exchange, Department of Chemistry, University of Indiana: Bloomington, IN, 1977.
(62) Bigeleisen, J.; Wolfsberg, M. *Adv. Chem. Phys.* **1958**, *1*, 15−76.

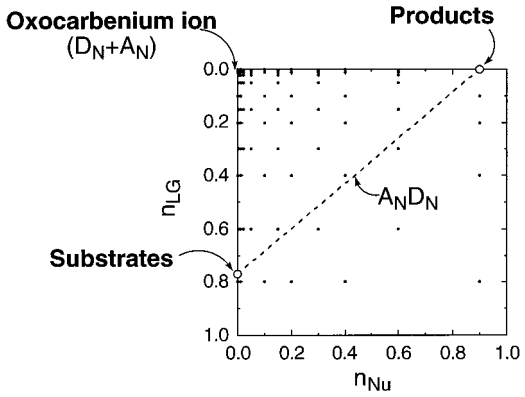

Figure 1. Reaction coordinate diagram. Positions in reaction coordinate space are illustrated by plotting the leaving group bond order (n_{LG}) on the ordinate and nucleophile bond order on the abscissa (n_{Nu}). Thus, the reaction proceeds from the substrates in the lower left corner to products in the upper right. A classical $D_N + A_N$ (S_N1) reaction mechanism involves formation of an oxocarbenium ion intermediate, with complete loss of the leaving group, before the nucleophile bond order starts to increase. A concerted, synchronous A_ND_N (S_N2) mechanism follows the dotted diagonal line, where the increase in n_{Nu} at each point matches exactly the loss of n_{LG}. Each point on the graph represents one of 85 trial transition state structures for which KIEs were predicted.

to calculate the individual bond orders from bond lengths and, from those, the force constants associated with each individual bond.

Structure Interpolation Method. Bond-vibrational modeling of transition states is usually accomplished by adjusting individual geometrical parameters until they match measured KIEs. This approach may not find the best or only solution and may include a solution that is chemically unreasonable. Enzyme-produced effects may be unrecognized since it is not clear what the expected KIEs are. Also, the modeling process is extremely time-consuming.

To address these difficulties, the structure interpolation approach was developed in which an algorithm describes the variation in molecular structure as a function of its position in reaction coordinate space (Figure 1) and generates trial transition state structures. In this way, all the geometrical parameters are varied at once in a systematic way. Predicted KIEs are calculated for each structure using BEBOVIB, and the one that most closely matches the experimental KIEs is selected.

In this approach, the structure of the ribosyl moiety of the transition state was assumed to vary between the first and second reference structures only as a function of its *oxocarbenium ion character* (OC). By definition, OC = 0 in the first reference structure, the reactant NAD^+ molecule, and OC = 1 in the second reference structure, the hypothetical oxocarbenium ion that would be the intermediate in a $D_N + A_N$ mechanism. The second reference structure also included the nicotinamide molecule. OC was a function only of the bond orders to the leaving group ($n_{LG,TS}$) and nucleophile ($n_{Nu,TS}$) in the transition state model and to the leaving group in the reactant ($n_{LG,react}$):

$$OC = 1 - (n_{Nu,TS} + n_{LG,TS})/n_{LG,react}$$

For example, to create a transition state model with $n_{LG,TS} = 0.1$ and $n_{Nu,TS} = 0.1$, if $n_{LG,react} = 0.8$, then OC = 0.75. According to this model, in a concerted, synchronous A_ND_N reaction where the loss of leaving group bond order equaled the increase in nucleophile bond order, the structure of the ribosyl moiety would not change at all in the course of the reaction, except at H1′.

Trial transition state structures were interpolated between the reactant NAD^+ and the {oxocarbenium ion + nicotinamide} structures as a function of a wide range of n_{LG} and n_{Nu} values; 85 structures with bond orders in the range 0.001−0.9 were used. In the initial model, each internal coordinate (bond length, bond angle, or dihedral angle) of the ribose ring was the linear combination of the first and second reference structures. For example, for a bond length in the ribosyl ring ($r_{ribosyl,TS}$)

$$r_{ribosyl,TS} = r_{ribosyl,react} + OC(r_{ribosyl,oxocarbenium} - r_{ribosyl,react}) \quad (1)$$

where TS, react, and oxocarbenium stand for transition state, reactant, and oxocarbenium ion, respectively.

The final method used a nonlinear combination of the reference structures in the ribose ring. To match the KIEs of nucleophilic substitutions on NAD^+ having higher $n_{LG,TS}$ and $n_{Nu,TS}$ than observed here, it was necessary to take transition state imbalance effects[63,64] into account. A common manifestation of transition state imbalance is that resonance stabilization of transition states occurs late in the reaction coordinate. In the case of NAD^+, resonance stabilization of the oxocarbenium ion by electron donation from O4′ and by hyperconjugation with the C2′−H2′ bond occurs late in oxocarbenium ion formation, with $n_{C1'-O4'}$, and $n_{C1'-C2'}$ becoming approximately exponential functions of OC. The results of ab initio calculations on model *N*-ribosides showed that $n_{C1'-O4'}$, which is diagnostic of the ribose ring in general, varied as a function of "$OC^{1.8}$", rather than "OC" in eq 1. This is close to the value of the exponent, "OC^2", predicted by Kresge (see refs 63 and 64). This will be fully described elsewhere. The hydrolysis reactions in this and the accompanying report had very high values of OC, so transition state imbalance effects were small, and the KIE data could be fit adequately using a linear treatment of internal coordinates. The nonlinear treatment was used, however, for the sake of consistency with future applications.

The internal coordinates within the nicotinamide ring were a function of $n_{LG,TS}$ only. For example, for a bond length in the nicotinamide ring ($r_{nic,TS}$)

$$r_{nic,TS} = r_{nic,react} + (1 - n_{LG,TS}/n_{LG,react})(r_{nic,nic} - r_{nic,react})$$

where $r_{nic,nic}$ is the corresponding bond length in the crystal structure of nicotinamide.[65]

The geometry of H1′ was not a function of OC only, since the bond angle ∠N1−C1′−H1′ would be affected by the relative bond orders of the nucleophile and the leaving group. An equation was used that takes into account the bond angles in the reactant, oxocarbenium ion, and product structures, as well as the higher tendency to planarity of the more sp^2-hybridized carbon of structures with high oxocarbenium ion character. The bond angle α, ∠N1−C1′−H1′, was adjusted according to the following equations:

$$\text{if} \quad n_{LG,TS} = n_{Nu,TS}, \quad \text{then} \quad \alpha = \alpha_{oxocarbenium}$$

$$\text{if} \quad n_{LG,TS} < n_{Nu,TS}, \quad \text{then} \quad \alpha = \alpha_{oxocarbenium} - (\alpha_{oxocarbenium} - \alpha_{r5p})[(n_{Nu} - n_{LG})/n_{r5p}](1 - OC)$$

(63) Bernasconi, C. F. *Adv. Phys. Org. Chem.* **1992**, *27*, 119−238.
(64) Richard, J. P. *Tetrahedron* **1995**, *51*, 1535−1573.
(65) Wright, W. B.; King, G. S. D. *Acta Crystallogr.* **1954**, *7*, 283−288.

$$\text{if} \quad n_{LG,TS} > n_{Nu,TS}, \quad \text{then} \quad \alpha = \alpha_{oxocarbenium} + (\alpha_{react} - \alpha_{oxocarbenium})[(n_{LG} - n_{Nu})/n_{react}](1 - OC)$$

where n_{r5P} is the C1′−O1′ bond order of the ADP-ribose molecule found in the X-ray crystallographic structure of liver alcohol dehydrogenase (PDB[66] structure: 5ADH). The angle α_{r5P} is the "∠N1−C1′−H1′ bond angle" [67] = 38.1°, optimized for the structure of the α-ribose-5-phosphate moiety of ADP-ribose from the 5ADH structure at the RHF/3-21G level of theory using the program Gaussian 94.[68]

CTBi. A computer program, CTBi (*C*artesian coordinates to *T*ransition state structures to *B*EBOVIB input using *i*nternal coordinates) was written to generate trial transition state models. It reads in structures in Cartesian coordinates, parses the structures to find leaving group and nucleophile atoms and to identify ring closures, converts the reference structures to an internal coordinate system, then generates a series of transition state structures based on a list of $n_{LG,TS}$ and $n_{Nu,TS}$ values, and writes out the structures in polar coordinates for input into BEBOVIB.

First Reference Structure: The Reactant State. The reactant state model of NAD^+ was from the X-ray crystallographic structure of the lithium salt of NAD^+,[69] truncated to nicotinamide mononucleotide with a monoanionic phosphate. Hydrogens were added and optimized at the RHF/6-31G** level. Unlike other (e.g., adenylyl) nucleotides,[70,71] the conformation of the ribose ring attached to the nicotinamide has a significant effect on bond orders. Since KIEs are a function of the *differences* in vibrational modes between the reactant and transition state structures, the reactant model is as important in determining the predicted KIEs as the transition state. In a comparison of five X-ray crystallographic structures of NAD^+ in the 3′-*endo* conformation[72] versus 4 structures in the 2′-*endo* conformation,[73] the 3′-*endo* structures had lower bond orders by 0.17 for C4′−O4′ and C1′−C2′, 0.15 for C1′−N1, and higher by 0.03 for C1′−O4′. These differences may arise partly from the anomeric effect in the 3′-*endo* conformation, where interaction of the lone-pair electrons of the ring oxygen antiperiplanar to the C1′−N1 bond would lead to a lengthening of the C1′−N1 and C4′−O4′ bonds and shortening of the C1′−O4′ bond. In the 2′-*endo* conformation, the angle between the C1′−N1 bond and the lone pair electrons is wider, leading to a weaker anomeric effect. Similar effects have been observed between axial and equatorial acetals and *O*-glucosides.[74]

In attempting to locate the transition state, no combination of $n_{LG,TS}$ and $n_{Nu,TS}$ could be found that matched the measured KIEs when using a 2′-*endo* reactant or a combination of 3′-*endo* and 2′-*endo* reactants (ribosyl rings, in general, have weak conformation preference in solution and would be expected to exist in a combination of states[75]). Only the 3′-*endo* reactant gave calculated KIEs that matched the measured KIEs. NMR spectra of NAD^+ and nicotinamide mononucleotide in solution indicate an unusual distribution of conformers skewed toward the 3′-*exo* and 2′-*exo* conformations,[76] with a predominance of the 3′-*exo* conformer.[77] These conformers have not been observed for pyridine nucleotides in the solid state but may be favored in solution because of electrostatic interactions between the anionic phosphate and the cationic aglycone. Like the 3′-*endo* conformer, the lone pair orbital of the ring oxygen is nearly antiperiplanar to the C1′−N1 bond in the 3′-*exo* and 2′-*exo* conformations. The bond lengths in the ribosyl ring of these conformers, and therefore the resulting KIEs, are expected to be closer to those produced using the 3′-*endo* conformer as the reactant model. In locating appropriate transition state structures, a model based on the 3′-*endo* conformer was required to match the measured KIEs, while the 2′-*endo* conformer as the reactant model did not provide agreement for any combination of $n_{LG,TS}$ and $n_{Nu,TS}$.

The 3′-*exo* and 2′-*exo* conformations would be expected to be more reactive than the 2′-*endo* conformer. Jones and Kirby[78] showed a correlation between C−O bond length and reactivity and estimated that the free energy of activation for unimolecular heterolysis decreased with increasing reactant bond length by 250 kcal·mol^{-1}·Å^{-1}. Assuming that the same effects obtain for C−N bonds and that the energies of activation are of the same magnitude, then given an average difference of $\Delta r_{C1'-N1} = 0.05$ Å, the free energy of activation for 3′-*endo* conformers would be 12.5 kcal·mol^{-1} lower than for 2′-*endo* conformations. However, when the different conformers are in rapid equilibrium in solution, the difference in reactivity will have no effect on the KIEs.

Second Reference State Structure: The Oxocarbenium Ion + Nicotinamide. The starting point to establish the structure of the oxocarbenium ion model was the X-ray crystallographic structure of ribonolactone.[79] The carbonyl oxygen was changed to hydrogen, a phosphate group derived from the NAD^+ structure was added, and all atoms were minimized at the RHF/6-31G** level, with minimal bond bend and torsional constraints added to prevent the anionic phosphate from forming a covalent bond with C1′. The nicotinamide molecule was the X-ray crystallographic structure,[65] with hydrogens added and optimized at the same level of theory.

Hyperconjugation at H2′. The Hartree−Fock method used for structure optimization is inherently unable to reflect the electron correlation effects necessary to model the hyperconjugation that is observed in the β-secondary (2′-^{3}H) KIE. Hyperconjugation arises from the interaction of the occupied π-symmetry orbital of the β-carbon, C2′, with the developing vacant p-orbital of the anomeric carbon as the leaving group departs[80] (Figure 2). This leads to a lengthening of the C2′−

(66) Bernstein, F. C.; Koetzle, T. F.; Williams, G. J. B.; Meyer, E. F., Jr.; Brice, M. D.; Rodgers, J. R.; Kennard, O.; Shimanouchi, T.; Tasumi, M. *J. Mol. Biol.* **1977**, *112*, 535−542.

(67) The angle between the C1′−H1′ bond and the normal to the plane defined by the atoms O4′, C1′, and C2′.

(68) Frisch, M. J.; Trucks, G. W.; Schlegel, H. B.; Gill, P. M. W.; Johnson, B. G.; Robb, M. A.; Cheeseman, J. R.; Keith, T.; Petersson, G. A.; Montgomery, J. A.; Raghavachari, K.; Al-Laham, M. A.; Zakrzewski, V. G.; Ortiz, J. V.; Foresman, J. B.; Cioslowski, J.; Stefanov, B. B.; Nanayakkara, A.; Challacombe, M.; Peng, C. Y.; Ayala, P. Y.; Chen, W.; Wong, M. W.; Andres, J. L.; Replogle, E. S.; Gomperts, R.; Martin, R. L.; Fox, D. J.; Binkley, J. S.; Defrees, D. J.; Baker, J.; Stewart, J. P.; Head-Gordon, M.; Gonzalez, C.; Pople, J. A. *Gaussian 94, Revision C.2*; Gaussian, Inc.: Pittsburgh, PA, 1995.

(69) Reddy, B. S.; Saenger, W.; Muhlegger, K.; Weimann, G. *J. Am. Chem. Soc.* **1981**, *103*, 907−914.

(70) Moodie, S. L.; Thornton, J. M. *Nucleic Acids Res.* **1993**, *21*, 1369−1380.

(71) Gelbin, A.; Schneider, B.; Clowney, L.; Hsieh, S. H.; Olson, W. K.; Berman, H. M. *J. Am. Chem. Soc.* **1996**, *118*, 519−529.

(72) Reference 69 and PDB[66] structures: 1GEU and 2NAD (two independent NAD^+ molecules per structure).

(73) PDB structures: 1HLD (two NAD^+ molecules), 2OHX, and 1LDM.

(74) Briggs, A. J.; Glenn, R.; Jones, P. G.; Kirby, A. J.; Ramaswamy, P. *J. Am. Chem. Soc.* **1984**, *106*, 6200−6206.

(75) Altona, C.; Sundaralingam, M. *J. Am. Chem. Soc.* **1973**, *95*, 2333−2344.

(76) Oppenheimer, N. J. In *The pyridine nucleotide coenzymes*; Everse, J., Anderson, B., You, K.-S., Eds.; Academic Press: New York, 1982; pp 51−89.

(77) Oppenheimer, N. J. In *Pyridine nucleotide coenzymes*; Dolphin, D., Poulson, R., Avramovic, O., Eds.; Wiley-Interscience: New York, 1987; pp 185−230.

(78) Jones, P. G.; Kirby, A. J. *J. Am. Chem. Soc.* **1984**, *106*, 6207−6212.

(79) Kinoshita, Y.; Ruble, J. R.; Jeffrey, G. A. *Carbohydr. Res.* **1981**, *92*, 1−7.

(80) Hehre, W. J. *Acc. Chem. Res.* **1975**, *8*, 369−376.

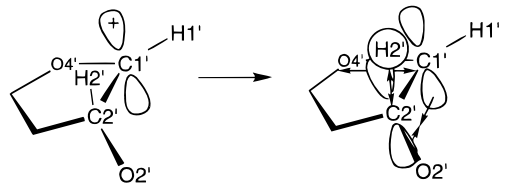

Figure 2. Hyperconjugation at H2′. Interaction of the vacant p-orbital of C1′ of the oxocarbenium ion with the occupied π-symmetry orbital of C2′ leads to C1′−C2′ π-bonding. Concomitant with increased $n_{C1'-C2'}$ are decreases in $n_{C2'-H2'}$ and $n_{C1'-O4'}$. This interaction leads to a large, normal 2′-^{3}H KIE.

H2′ bond, which in turn causes the large 2′-^{3}H KIE. As would be expected, the 2′-^{3}H KIEs predicted from the Hartree−Fock optimized structure were much lower (approximately 1.02) than the measured KIEs for oxocarbenium ion-like transition states. Hyperconjugation was incorporated by adjusting the oxocarbenium ion structure. Decreasing $n_{C2'-H2'}$, with an equal increase in $n_{C1'-C2'}$, and decrease in $n_{C1'-O4'}$ conserved the total bond order to C1′ and accounted for hyperconjugation. Decreasing $n_{C2'-H2'}$ in the oxocarbenium ion by 0.059 gave a predicted 2′-^{3}H KIE that matched the measured KIE. These changes had no effect on the predicted 1′-^{14}C and 1-^{15}N KIEs since the total bond order to C1′ did not change. The predicted 4′-^{18}O KIE became less inverse due to the decrease in $n_{C1'-O4'}$, more closely matching the measured KIE. The 2′-^{3}H KIE for diphtheria toxin-catalyzed hydrolysis was successfully predicted using the same extent of hyperconjugation.[5]

BEBOVIB Calculations. KIEs were calculated with BEBOVIB, using a cutoff model of the reference structures that included all atoms within two bonds of the isotopic labels, giving a "highly proper" [51] cutoff model. KIEs were calculated for all isotopic labels using the same cutoff model. The cutoff models were the input for the program CTBi. The internal coordinates used in the BEBOVIB calculations were similar to those used by Horenstein et al.,[15] but with bond stretching and bond angle bending force constants taken from the AMBER force field of Kollman's group[81] after conversion to appropriate units. Torsional force constants were from Vasko et al.[82]

The reaction coordinate for a bimolecular (A_ND_N) reaction was generated by coupling the C1′−N1 and C1′−O bond stretches with an interaction force constant of 1.1, such that the asymmetric N1−C1′−O stretch had a negative force constant.[7] This creates the reaction coordinate, a normal mode with an imaginary frequency. Inversion of the anomeric carbon was effected by coupling the C1′−N1 and C1′−O bond stretches to bond angle bends X−C1′−Y, where X = N1 or O and Y = C2′, O4′, or H1′, with interaction force constants of + or −0.05.[83] The reaction coordinate for a $D_N + A_N$ reaction was generated by giving the C1′−N1 bond stretch a small, negative force constant, −0.005 mdyn/Å, which gave rise to an imaginary frequency that was the reaction coordinate. Inversion of the anomeric carbon was as above. For a transition state involving nucleophilic attack onto an oxocarbenium ion, the reaction coordinate was created as for a $D_N + A_N$ reaction, but with the C1′−O bond stretch having the negative force constant.

Results

Primary, α-secondary, β-secondary, and remote KIEs were measured by the ^{3}H/^{14}C competitive label method, as described previously[2] (Table 1). The ring oxygen, 4′-^{18}O, KIE was determined by mass spectrometric analysis as described in the following paper.[5] At 100 °C and pH 4.0, NAD^+ is hydrolyzed exclusively to ADP-ribose and nicotinamide with a rate constant of $k = 5.3\ (\pm\ 0.7) \times 10^{-4}\ s^{-1}$. The rate was unaffected by varying [NaOAc] from 0.01 to 1.0 M (not shown), showing that there is neither a salt effect nor general base catalysis.

Table 1. Kinetic Isotope Effects on Hydrolytic Solvolysis of NAD^+ at 373 K

label of interest	KIE type	exptl KIE (± 95% CI)[a]	n[b]	predicted KIE at transition state[c]
1-^{15}N[d]	primary, leaving group	1.020 ± 0.007	8	1.020
1′-^{14}C[e]	primary, anomeric carbon	1.016 ± 0.002	8	1.019
1-^{15}N,1′-^{14}C[f]	double primary	1.034 ± 0.002	6	
1′-^{3}H[g]	α-secondary	1.194 ± 0.005	5	1.198
2′-^{3}H[g]	β-secondary	1.114 ± 0.004	7	1.114[h]
4′-^{3}H[g]	γ-secondary	0.997 ± 0.001	3	−
5′-^{3}H[g]	δ-secondary	1.000 ± 0.003	10	−
4′-^{18}O[i]	α-secondary	0.988 ± 0.007	3	0.986

[a] Experimental KIEs determined by P.J.B. and Kathleen A. Rising. The KIEs reported for this reaction in Rising and Schramm[2] were based on most of the same data but were "normalized" to 310 K for comparison with cholera toxin-catalyzed hydrolysis. The KIEs reported here are the experimental KIEs as measured for the reaction at 373 K. [b] Number of independent, quadruplicate determinations. [c] $n_{LG,TS} = 0.02$ and $n_{Nu,TS} = 0.005$. [d] Labeled substrate: [1-^{15}N,5′-^{14}C]NAD^+. Remotely labeled substrate: [4′-^{3}H]- or [5′-^{3}H]NAD^+. [e] Remotely labeled substrate: [4′-^{3}H]- or [5′-^{3}H]NAD^+. [f] Labeled substrate: [1-^{15}N,1′-^{14}C]NAD^+. Remotely labeled substrate: [4′-^{3}H]- or [5′-^{3}H]NAD^+. [g] Remotely labeled substrate: [5′-^{14}C]- or [8-$^{14}C_A$]NAD^+, in the adenine ring. [h] Hyperconjugation was modeled by making the predicted 2′-^{3}H KIE match the experimental KIE exactly. [i] Measured by positive-ion whole-molecule mass spectrometry. Labeled substrate: [4′-^{18}O]NAD^+.

The measured 1′-^{3}H KIE = 1.194 ± 0.005 is somewhat larger than the previously reported 1′-^{2}H KIEs for pH-independent hydrolysis of NAD^+,[17] NMN^+,[17] and nicotinamide riboside[18] at 25 °C when the Swain−Schaad relationship is used to convert ^{2}H to ^{3}H KIEs[84] and a temperature correction applied.[85] Previous reports gave ^{3}H-equivalent isotope effects of 1.12, 1.16, and 1.17, respectively. Both the Swain−Schaad and temperature corrections are approximate, and significantly lower measured KIEs are observed without full correction of the KIEs to 0% reaction.[86] Thus, the measured 1′-^{3}H KIE is in reasonable agreement with previous measurements.

The error range for the measured KIEs is reported as the 95% confidence interval (CI). Isotope effects on ^{3}H or ^{14}C, where the opposite label was used as the remote reporter, gave confidence intervals of ±0.001 to ±0.005. Despite having eight independent quadruplicate determinations, the error range for the 1-^{15}N KIE, 0.007, was greater than that of the other KIEs and that of the diphtheria toxin-catalyzed hydrolysis of NAD^+ (1-^{15}N KIE = 1.030 ± 0.004).[5,85] The reason for this variability in the measured KIE is not known. To confirm the accuracy of the value, the double primary [1-^{15}N, 1′-^{14}C]NAD^+ KIE was also measured. As required, the product of the individual 1′-^{14}C and 1-^{15}N KIEs, 1.036, is within experimental error of the measured double [1′-^{14}C,1-^{15}N] KIE, 1.034 ± 0.002. This measurement was made with a good confidence interval and confirmed the value of 1.020 for the 1-^{15}N KIE. The 4′-^{18}O KIE determined by the dual-remote radiolabel technique also had a high variability, 0.984 ± 0.024 after four independent

(81) Cornell, W. D.; Cieplak, P.; Bayly, C. I.; Gould, I. R.; Merz, K. M., Jr.; Ferguson, D. M.; Spellmeyer, D. C.; Fox, T.; Caldwell, J. W.; Kollman, P. A. *J. Am. Chem. Soc.* **1995**, *117*, 5179−5197.
(82) Vasko, P. D.; Blackwell, J.; Koenig, J. L. *Carbohydr. Res.* **1972**, *23*, 407−416.
(83) Markham, G. D.; Parkin, D. W.; Mentch, F.; Schramm, V. L. *J. Biol. Chem.* **1987**, *262*, 5609−5615.
(84) ^{3}H-KIE = (^{2}H-KIE)$^{1.44}$.
(85) $KIE_{373\ K} = \exp[(298/373)\ \ln(KIE_{298\ K})]$.
(86) Northrop, D. B. *Annu. Rev. Biochem.* **1981**, *50*, 103−131.

quadruplicate determinations. The similarity of the average KIE, 0.984, to the KIE determined by mass spectrometry, 0.988 ± 0.007, must be considered fortuitous in light of the error range and is not included in Table 1.

Discussion

The KIEs of NAD^+ hydrolysis clearly indicate an oxocarbenium ion-like transition state. The primary ^{15}N KIE indicates significant, but not complete, C1′−N1 bond cleavage at the transition state. The small primary 1′-^{14}C KIE indicates low bond order to the approaching nucleophile, and the large, normal secondary 1′-^{3}H and 2′-^{3}H KIEs, along with the inverse secondary 4′-^{18}O KIE, are consistent with an oxocarbenium ion-like transition state.

Mechanism and Oxocarbenium Ion Lifetime. The kinetic scheme in eq 2 shows possible routes for NAD^+ hydrolysis,

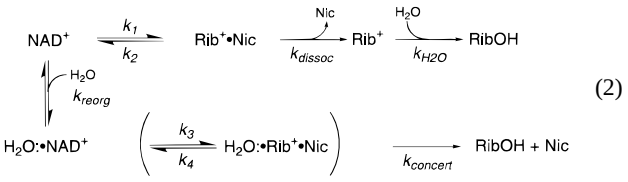

(2)

where Rib^+ is the ribo-oxocarbenium ion of ADP-ribose, RibOH is the product ADP-ribose, and Nic is product nicotinamide. The upper pathway is for a $D_N + A_N$ mechanism, while the bottom pathway is for an A_ND_N mechanism. Whether a neutral/ion/neutral "sandwich" (H_2O·Rib^+·Nic) occurs on the A_ND_N pathway cannot be determined by chemical or KIE evidence. Nucleophilic association and attack on the ion/neutral complex (Rib^+·Nic) was not considered since the rate of nucleophile association is lower than k_{dissoc}[23,87,88] .

Nucleophilic substitution reactions of glycosides and related compounds have been consistently[23,24,27,89] observed to proceed through transition states with substantial oxocarbenium ion character in the glycone. These reactions exist on the borderline between $D_N + A_N$ (S_N1) and A_ND_N (S_N2) mechanisms. The experimentally determined Brønsted coefficients, β_{LG}, of −1.1 for enzymatic[35,42] and −0.9 for nonenzymatic[35] NAD^+ hydrolyses indicate a dissociative, oxocarbenium ion-like transition state that could arise from either a $D_N + A_N$ or an asynchronous A_ND_N mechanism.

In the analysis of Jencks,[90,91] the rate-determining step, and therefore the structure of the transition state, depends on the stability of the oxocarbenium ion, whether it has a real existence in solution. If the oxocarbenium ion is stable enough for it to separate diffusionally from nicotinamide (approximately 10^{-10} s), then the reaction becomes stepwise, a $D_N + A_N$ reaction. Chemical evidence in the literature rules this out in the case of NAD^+ hydrolysis. For this mechanism, product partitioning would show high selectivity between nucleophiles and give a mixture of inversion and retention of configuration at the anomeric carbon since the nucleophile could approach the solvent-equilibrated oxocarbenium ion from either direction. Experimentally, nucleophilic substitutions of pyridine nucleotides are highly or completely insensitive to the nature of the nucleophile; for example, for nucleophilic substitutions on NAD^+, the products partition as a function of the molar ratios of water and methanol rather than their nucleophilicities.[38] There is no experimental evidence on the stereochemistry of hydrolysis, but methanolysis gives a ratio of inversion:retention of the anomeric carbon of 22(± 2):1[39] in the pH-independent range, implying that the oxocarbenium ion does not diffuse away before the nucleophilic attack. The 330-fold decrease in the rate of hydrolysis of a riboside analogue with a bulky substituent that prevents "backside" solvation[25] argues for preassociation of the nucleophile and against a $D_N + A_N$ mechanism.

The chemical evidence favors the preassociation of the water nucleophile with NAD^+(k_{reorg}), followed by a concerted, asynchronous nucleophilic displacement of nicotinamide ($k_{concert}$), giving an A_ND_N mechanism. In this case, the reaction will have low selectivity between nucleophiles, and it will go with inversion of configuration at the anomeric carbon (i.e., β-NAD^+ to α-ADP-ribose). Even though NAD^+ is surrounded by water, a significant amount of entropy must be lost from bulk water to reorganize and preassociate with NAD^+. This is reflected by the inclusion of k_{reorg}. The chemical evidence against a $D_N + A_N$ mechanism (cited above) are all consistent with an asynchronous A_ND_N mechanism.

Transition State Structure. Transition State Structure and Mechanism. In the BEBOVIB analysis of KIEs, three reaction coordinate motions are possible: (1) cleavage of the C1′−N1 bond without nucleophile participation (unimolecular dissociation), (2) attack of the nucleophile on C1′,[92] and (3) concerted approach of the nucleophile and departure of the leaving group. In the latter case, the reaction is concerted.

The chemical evidence against a $D_N + A_N$ mechanism was supported by the difficulty in matching the KIEs for a unimolecular dissociation reaction coordinate. First, if an oxocarbenium ion intermediate existed, then the primary ^{15}N KIE for complete cleavage of the C1′−N1 bond would have to be at the equilibrium limit of 1.027,[93−95] greater than the measured KIE of 1.020.[96] The experimental 1-^{15}N and 1′-^{14}C KIEs could be reproduced for $n_{LG,TS} \approx 0.2$, with a solvating water (not in the reaction coordinate) in the place of the nucleophile, with bond order to C1′ ≈ 0.15. This combination of bond orders reduces the oxocarbenium ion character of the predicted transition state and makes it impossible to match any of the 1′-^{3}H (calculated KIE = 1.010), 2′-^{3}H (1.065), or 4′-^{18}O (0.995) secondary KIEs. Also, this would be inconsistent with such chemical evidence as the high β_{LG} of hydrolysis.

An excellent match of predicted and measured KIEs for an A_ND_N mechanism was found, with $n_{LG,TS} = 0.02$ and $n_{Nu,TS} = 0.005$ (Figure 3, Table 1, Table S1 (Supporting Information)).

(87) Amyes, T. L.; Jencks, W. P. *J. Am. Chem. Soc.* **1989**, *111*, 7900−7909.

(88) Richard, J. P. *J. Org. Chem.* **1992**, *57*, 625−629.

(89) Jones, C. C.; Sinnott, M. L.; Souchard, I. J. L. *J. Chem. Soc., Perkins 2* **1977**, 1191−1198.

(90) Jencks, W. P. *Acc. Chem. Res.* **1980**, *13*, 161−169.

(91) Jencks, W. P. *Chem. Soc. Rev.* **1981**, *10*, 345−375.

(92) This is not chemically reasonable since it would require (unreasonably) that the leaving group be present, but not in the reaction coordinate. If the leaving group has diffused away, then the irreversible step has occurred and the correct reaction coordinate motion is unimolecular dissociation (above). For this reason, this mechanism will not be considered further.

(93) The semiclassical limit for an ^{15}N KIE for loss of a full bond order is 1.035 at 100 °C,[94] but given the low leaving group bond order in the reactant, $n_{LG} = 0.77$, and the increase in the ring N−C bond orders in the product nicotinamide compensating for loss of the C1′−N1 bond, the limit for this reaction is smaller. The equilibrium isotope effect (EIE) on 1-^{15}N for protonation of 3-acetylpyridine was 1.019.[95] The prediction that EIEs for methyl transfer would be 0.6% higher gives a predicted EIE of 1.025 for methylation of 3-acetylpyridine. This is very similar to the 1-^{15}N EIE = 1.027 predicted here.

(94) Huskey, W. P. In *Enzyme mechanism from isotope effects*; Cook, P. F., Ed.; CRC Press Inc.: Boca Raton, FL, 1991; pp 37−72.

(95) Kurz, J. L.; Pantano, J. E.; Wright, D. R.; Nasr, M. M. *J. Phys. Chem.* **1986**, *90*, 5360−5363.

(96) Although it could risk becoming circular logic to judge possible transition state models on the basis of the measured KIEs when one of the stated purposes of the study is to test the methods of modeling transition structures from KIEs, the magnitudes of the effects invoked here and in the next paragraph are large enough that the details of the model will not affect these arguments.

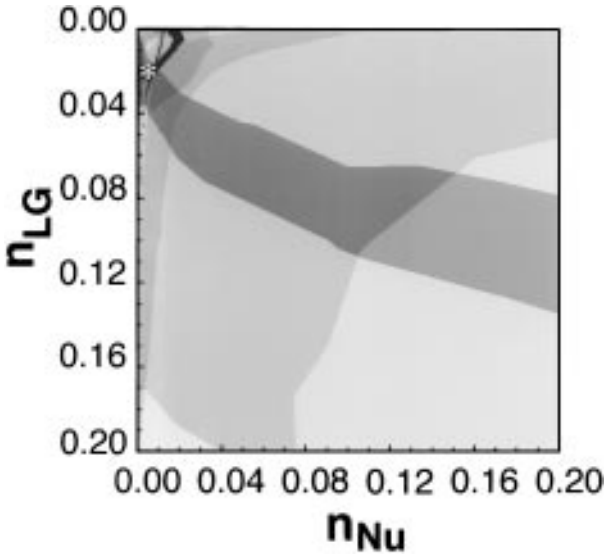

Figure 3. Match of predicted versus experimental KIEs. For each isotopic label, the colored area represents the match of the predicted with the experimental KIEs as a function of n_{LG} and n_{Nu} in the type reaction coordinate diagram. The light shading represents the 95% confidence interval of each measured KIE, with dark shading representing the exact measured KIE (approximately ± 0.001): blue, 1-^{15}N; red, 1′-^{14}C; gray, 1′-^{3}H; green, 2′-^{3}H; orange, 4′-^{18}O. The predicted transition state structure is indicated by *. Only the top left (dissociative) corner of reaction coordinate space is shown.

The shaded bands in Figure 3 show the structures in reaction coordinate space where the KIEs predicted by the program BEBOVIB match the experimental KIEs. Because of the shapes of the areas where the predicted and experimental KIEs match, the location of the best match in reaction coordinate space is unambiguous. The predicted 1-^{15}N KIE matches the experimental KIE exactly. So does the 2′-^{3}H KIE, because the extent of hyperconjugation was selected to match the experimental KIE. The predicted 4′-^{18}O and 1′-^{3}H KIEs are within the 95% CI of the experimental ones. Only the predicted 1′-^{14}C KIE = 1.019 falls outside the experimental range 1.016 ± 0.002. Considering that this is a primary KIE, with large changes in bond orders and angles occurring at this center, such a small discrepancy is quite acceptable.

The experimental KIEs are qualitatively consistent with an oxocarbenium ion-like transition state and are similar to those determined previously for other nucleophilic substitutions of glycosides. The 1′-^{3}H KIE is close to that observed for other *N*-riboside hydrolyses[7,15,44,45,47,49] and indicates a highly dissociative transition state structure. A more concerted reaction would be expected to have a more sterically crowded environment at the 1′-^{3}H, and therefore a lower KIE. The size of the 2′-^{3}H KIE clearly indicates hyperconjugation of the C2′−H2′ bond with C1′ (Figure 2) and is close to KIEs observed for other *N*-riboside hydrolyses[7,15,45,47−49] and for hydrolyses of gluco-[11] and sialylglycosides.[10] The magnitude of hyperconjugation, as distinct from inductive effects, depends strongly on the angle between the C2′−H2′ bond and the p-orbital on C1′, being maximal when they are eclipsed or anti and zero when the angle is 90°.[97,98] In the oxocarbenium ion, resonance stabilization within the ribose ring results in atoms C4′−O4′−C1′−C2′ being coplanar. As a result, the only available ring conformations are C3′-*endo* and C3′-*exo*. In the 3′-*endo* conformation, the N1−C1′−C2′−H2′ dihedral angle is −59.8°, versus 0.1° in the 3′-*exo* conformation. Given the angular dependence of hyperconjugation,[97,98] a 2′-^{3}H KIE as large as observed here can only occur with a 3′-*exo* conformer; that is, the conformation of the oxocarbenium ion is constrained by the magnitude of the 2′-^{3}H KIE to be 3′-*exo*. The 4′-^{18}O KIE = 0.988 is similar to that measured for the ring oxygen, 0.991, during hydrolysis of methyl β-glucoside.[11] It is inverse because the environment of the ring oxygen becomes more vibrationally restricted by the increase in $n_{C1'-O4'}$ from 0.96 in the reactant to 1.73 in the transition state.

The structure of the ribosyl moiety in the transition state changes in response to the loss of bond order to C1′ and its rehybridization toward planar sp^2 (Figure 4a). The ring atoms C4′−O4′−C1′−C2′ become coplanar because of the increased double-bond character in the O4′−C1′ and C1′−C2′ bonds. The bond order $n_{C1'-O4'}$ increases by 0.77, due largely to resonance stabilization of the increased positive charge on C1′; $n_{C1'-C2'}$ increases by 0.23 due to inductive effects and hyperconjugation; $n_{C2'-H2'}$ decreases by 0.032 due to hyperconjugation. The bond order $n_{C1'-H1'}$ increases by 0.023, but the tendency of the higher bond order to give an inverse KIE is offset by the decreased out-of-plane bending force constants to give the large measured 1′-^{3}H KIE = 1.194. Bond orders within the nicotinamide ring also change as it proceeds from a formally positive nitrogen in the reactant to being neutral in the nicotinamide product. The n_{N1-C2} and n_{N1-C6} bond orders of the nicotinamide increase by a total of 0.065.

The electrostatic potential surface reflects changes in the electron distribution of the molecule (Figure 4b). With the loss of the C1′−N1 bond, the nicotinamide ring becomes neutral and the positive charge is localized in the ribosyl ring at the transition state. The formal positive charge in the reactant (left structure) appears as regions of positive (red) electrostatic potential delocalized throughout the nicotinamide ring and into the ribosyl ring. In the transition state, that charge is localized into the ribosyl ring, as is visible in the structure of the transition state without the water nucleophile (mid-left). The protons of the water nucleophile in the transition state (mid-right) appear more electropositive than isolated water (right), reflecting polarization of the oxygen during nucleophilic attack.

Other Chemical Evidence. The concerted asynchronous transition state is consistent with all of the chemical evidence cited above. It is also consistent with other observations: (1) The rate of NAD$^+$ hydrolysis is pH-independent at pH < 6.5.[38] With such a low bond order to the electrophile at the transition state, the nucleophile will have a lower energy as a neutral water molecule, than as a hydroxide ion. (2) The entropy of activation of NAD$^+$ hydrolysis is low; with reported values of $\Delta S^{\ddagger} = -3.5 \pm 2.5$ cal/(mol·K)[38] and −0.54 cal/(mol·K),[41] traditionally considered a sign of a unimolecular dissociation or a "loose" transition state structure.[99] (3) A semiempirical study of the gas phase transition state of nicotinamide riboside hydrolysis suggested a highly oxocarbenium ion-like transition state structure.[100] As discussed by the authors of that study, hydrogen bonding is observed between the nucleophilic water and 2′-OH, which contributes to the higher predicted $n_{Nu,TS}$ in that study than determined here. (4) Studies of nucleophilic substitutions with numerous *N*- and *O*-pyranosyl and furanosyl glycosides have constantly indicated reaction mechanisms near the border between A_ND_N and $D_N + A_N$.[23,24,27,89] Again, NAD$^+$ hydrolysis is consistent with this rule.

(97) Sunko, D. E.; Szele, I.; Hehre, W. J. *J. Am. Chem. Soc.* **1977**, *99*, 5000−5004.
(98) Schramm, V. L. In *Enzyme mechanism from isotope effects*; Cook, P. F., Ed.; CRC Press Inc.: Boca Raton, FL, 1991; pp 367−388.
(99) Jencks, W. P. *Catalysis in chemistry and enzymology*; McGraw-Hill: New York, 1969.
(100) Schroder, S.; Buckley, N.; Oppenheimer, N. J.; Kollman, P. A. *J. Am. Chem. Soc.* **1992**, *114*, 8232−8238.

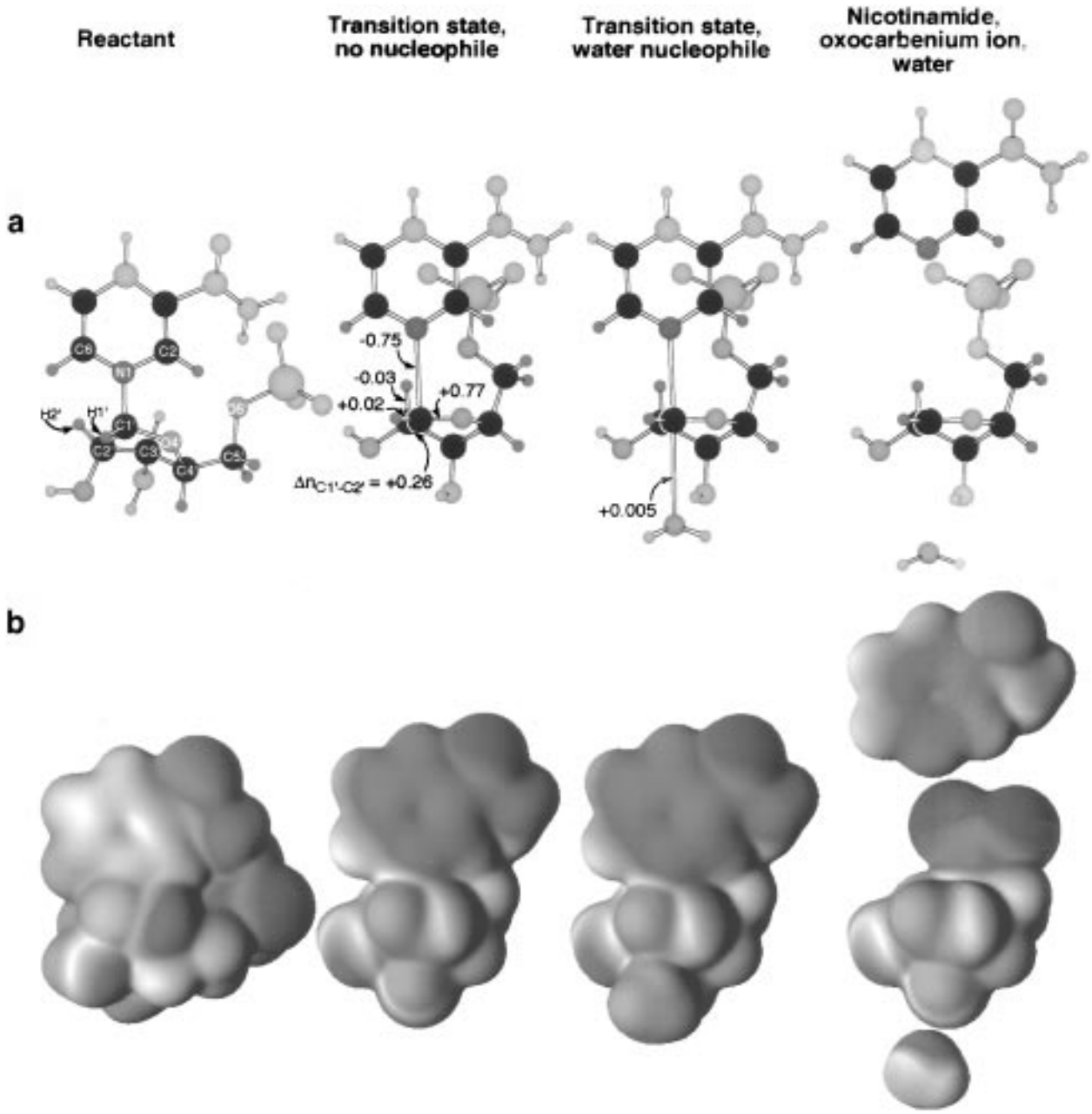

Figure 4. Structures of reactant, transition state with and without the water nucleophile, and the hypothetical oxocarbenium ion, with independent, noninteracting nicotinamide and water molecules. **(a)** Atoms present in the cutoff models used in BEBOVIB calculations are colored by element; all others are colored gray. Changes in bond order between the reactant and the transition state are indicated. All atoms within two bonds of the isotopically labeled positions were included in KIE predictions, yielding "highly proper" cutoff models.[51] **(b)** Electrostatic potentials projected onto the molecular surfaces of the full molecules in the same orientation as in part a, with *red* representing *positive* electrostatic potential and *blue* representing *negative* potential. Calculations were done at the RHF/6-31G** level. Molecular surfaces are at an electron density of 0.002 *e*/bohr^3, and the electrostatic potential spectrum is from −0.1 (blue) to 0.1 hartree/*e* (red).

Transition State Structure and $\sum n_{C1'}$. The total bond order to C1′ in the transition state structure, $\sum n_{C1',TS} = 3.92$, is higher than in the reactant, $\sum n_{C1',react} = 3.62$. This stems from the fact that the structure of the transition state was interpolated between the reactant and the ab initio optimized oxocarbenium ion, which had $\sum n_{C1',oxcarbenium} = 3.98$. This counterintuitive result was also observed in the transition state structures of NAD^+ hydrolysis catalyzed by cholera,[2] pertussis,[4] and diphtheria[5] toxins. The cholera and pertussis toxin transition states were modeled using the "ad hoc" method, without using quantum chemically derived reference structures for guidance. In those cases, it was possible to match the predicted to the measured KIEs only by having $\sum n_{C1',TS}$ higher than $\sum n_{C1',react}$. The same effect is seen for the oxocarbenium ion optimized using an hybrid density functional theory minimization using Becke's exchange functional[101] and Perdew and Wang's correlation functional[102] with the 6-31+G** basis set, where $\sum n_{C1',TS} = 3.82$.

The *increase* in $\sum n_{C1'}$ in a *dissociative* transition state structure is explained by consideration of the molecular orbitals involved (Figure 5) and by inductive effects. In reactant NAD^+, the region of the anomeric carbon, C1′, is electron deficient relative to the ring oxygen, O4′. This can be compensated for only by forming a stronger σ-bond since the sp^3 hybridization of C1′ is maintained by the C1′−N1 bond. There are (evidently) limits to how much shorter the C1′−O4′ bond can be made. In the oxocarbenium ion, however, C1′ becomes sp^2-hybridized and the empty p-orbital can form a π-bond with O4′, which

(101) Becke, A. D. *Phys. Rev. A* **1988**, *38*, 3098−3100.
(102) Perdew, J. P.; Wang, Y. *Phys. Rev. B* **1992**, *45*, 13244.

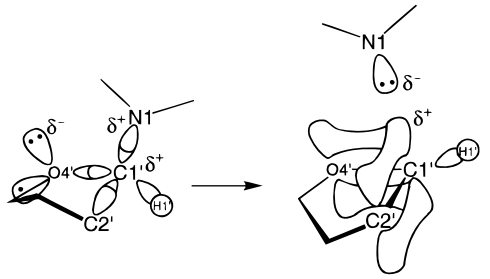

Figure 5. Rearrangement of molecular orbitals going from reactant NAD^+ to an oxocarbenium ion. π-Bonds are shown in red; all other molecular orbitals are in blue. The anomeric carbon, C1′, goes from sp^3 to sp^2 hybridization. In the oxocarbenium ion, rehybridization of the ring oxygen, O4′, allows formation of a π-bond. Hyperconjugation of the C2′−H2′ bond with the C1′ p-orbital allows C1′−C2′ π-bonding.

also has increased sp^2 character due to the increased $n_{C1'-O4'}$. Hyperconjugation of the C2′−H2′ bond with the C1′ p-orbital also contributes π-bonding. Second, the positive charge that, in the reactant, is delocalized into the nicotinamide ring becomes localized onto the ribosyl ring of the oxocarbenium ion. This leads to a further increase in $\sum n_{C1',TS}$ from inductive effects. Even though the result that $\sum n_{C1',TS} > \sum n_{C1',react}$ was counterintuitive, it was required to the match the measured KIEs in four hydrolytic reactions of NAD^+ and was further confirmed in this study with the ab initio optimized structure of the oxocarbenium ion and the transition state structure derived from that reference structure.

Nucleophile Bond Order. The selection of a transition state with a concerted, asynchronous reaction coordinate was based on (a) chemical evidence for an A_ND_N and strongly against a $D_N + A_N$ mechanism, (b) KIE evidence, where the experimental KIEs could not be fit to a unimolecular dissociation mechanism, but did fit well to a concerted reaction coordinate. Although the nucleophile bond order is small at the transition state, 0.005, its presence is necessary to match the experimental KIEs. Because KIEs are roughly an exponential function of bond order, a bond order of 0.005 is significantly different from 0.000. For example, with $n_{LG,TS} = 0.02$ and the nucleophile removed, the predicted KIEs are 1-^{15}N = 1.026 and 1′-^{14}C = 1.026, compared with the experimental KIEs of 1.020, and 1.016, respectively, and 1.020 and 1.019 for the A_ND_N transition state.

Calculated KIEs are a function not only of the structure of the transition state, but also of the reaction coordinate motion. If the concerted reaction coordinate is changed to a unimolecular dissociation while maintaining $n_{LG,TS} = 0.02$ and $n_{Nu,TS} = 0.005$,[103] the calculated KIEs change significantly to 1-^{15}N = 1.026 and 1′-^{14}C = 1.015. As stated above, the best fit to the 1-^{15}N and 1′-^{14}C KIEs for a unimolecular dissociation occurred at $n_{LG,TS} \approx 0.2$ and bond order to a solvating water ≈ 0.15, where the secondary KIEs could not be matched.

This is not to say, however, that all the bond orders are determined to within ± 0.005. Another consequence of the roughly exponential relationship between bond order and KIE is that KIEs are more sensitive to the *proportional* change in bond order rather than the *absolute* value of the change. For example, with $n_{LG} = 0.02$, increasing n_{Nu} from 0.005 to 0.01 gives an increase of 0.004 in the 1′-^{14}C KIE, while a change from $n_{LG} = 0.8$ to 0.805 gives a negligible change of 0.000 08.

As to the physical meaning of such a low nucleophile bond order, it is worth noting that KIEs are caused by *changes* in the forces experienced by an atom between two states, the reactant and transition state. Although both the reactant and transition state are surrounded by solvating water molecules, they are not included explicitly in the model because their position would not be able to reequilibrate during the reaction. The exception is the water molecule that enters the reaction coordinate and becomes the nucleophile. The estimated $n_{Nu,TS} = 0.005$ at the transition state represents the *increase* in interaction between the nucleophilic water and NAD^+ between the reactant and the transition state. To illustrate the point, if the nucleophilic water is present with an unreasonably high bond order of 0.1 to C1′ of the reactant structure (and therefore $n_{Nu,TS} \approx 0.105$ in the transition state), only small changes in the transition state structure occur. Even though $n_{Nu,TS}$ is small, it was not possible to match the experimental KIEs without including the water nucleophile.

Transition State Determination from KIEs by Structure Interpolation. Reliability of the Transition State Structure. The reliability of transition state structures derived from KIEs are difficult to assess since KIEs provide information that is not readily available from other methods (e.g., linear free energy relationships, enzyme inhibition constants for transition state analogues). One source of confidence is when the KIEs force the use of structures that can be shown by other means to be chemically reasonable. This was observed in two aspects of modeling the transition state structure of NAD^+ solvolytic hydrolysis. As discussed above, it was necessary to use the 3′-*endo* conformer in the reactant instead of the 2′-*endo* conformer in order to match the predicted and measured KIEs. In the second case, the previously counterintuitive result that $\sum n_{C1'}$ increases from the reactant to a dissociative transition state, a conclusion enforced by the KIEs, was supported by ab initio methods.

The Structure Interpolation Method. One of the goals of this study was to develop a systematic method of transition state determination. Using this method, we have determined transition state structures for NAD^+ solvolytic hydrolysis and for NAD^+ hydrolysis by diphtheria toxin.[5] Transition state structures have also been determined for cholera and pertussis-toxin catalyzed hydrolyses and ADP-ribosylation reactions (unpublished results and ref 46).

The method is conceptually simple, using only the following inputs: (a) The first reference structure: the X-ray crystallographic structure of NAD^+ with hydrogens added and optimized. (b) The second reference structure: the optimized structure of the hypothetical oxocarbenium ion intermediate, plus the X-ray crystallographic structure of nicotinamide with hydrogens added. (c) Hyperconjugation effects were modeled by decreasing $n_{C2'-H2'}$ in the second reference structure, with a concomitant decrease in $n_{C1'-O4'}$ and increase in $n_{C1'-C2'}$, until the predicted 2′-^{3}H KIEs matched the measured KIE.

Trial transition state structures are interpolated between the reference structures as a function of only the oxocarbenium ion character, OC, for the ribosyl moiety; the leaving group bond order, n_{LG}, for bonds within the leaving group; and a simple equation to describe the bond angle ∠N1−C1′−H1′. Judged on the basis of consistency and simplicity, the structure interpolation approach to transition state determination is preferred over previous methods.

Conclusion

KIEs measured for the solvolytic hydrolysis of NAD^+ in the pH-independent region were used to determine the transition state structure. The mechanism is concerted and asynchronous, A_ND_N, with a highly dissociative, oxocarbenium ion-like transition state structure. The remaining bond order to the leaving

(103) If the water nucleophile is removed from the reaction coordinate, it becomes a solvating water.

group nicotinamide, $n_{LG,TS}$, is 0.02, and the bond order to the approaching nucleophile, $n_{Nu,TS}$, is 0.005.

The increase in total bond order to the anomeric carbon between the reactant and the dissociative transition state structure was supported by ab initio optimizations of the hypothetical oxocarbenium ion. Increased bond order to C1′ has now been observed in four NAD^+ hydrolytic reactions.

The transition state was identified using a structure interpolation approach that automatically generates trial transition state structures by interpolating between reactant and oxocarbenium ion reference structures. The transition state with predicted KIEs that most closely match the experimental KIEs is selected. The ability to model the solvolytic hydrolysis and the agreement between the solvolytic transition state and chemical characterization of the reaction support the validity of this approach. The same method has been used to model the diphtheria toxin-catalyzed hydrolysis.[5] Using this method, the transition state structures for other nucleophilic substitutions of *N*-ribosides will be modeled.

The use of electronic structure methods and the creation of a modeling method based on structure interpolation represent an attempt to rationalize the measured KIEs and to create a theoretical framework within which a whole family of nucleophilic substitution reactions of *N*-ribosides can be placed. It is hoped that the details of this model will shed light on the reaction mechanism and on how enzymes use binding energy to promote catalysis. A better understanding of how these enzymes work will improve our ability to harness this binding energy to promote other reactions or to inhibit them.

Acknowledgment. We thank Mr. Edward Nieves and Dr. Ruth H. Angeletti for their invaluable help in developing the method of mass spectrometric determination of KIEs and Dr. Michael Sinnott for providing the precursor for synthesis of [4′-^{18}O]NAD^+. KIEs by the radiolabel method were determined in cooperation with Dr. Kathleen A. Rising. We thank Dr. John Richard of SUNY Buffalo for his thoughtful reading and helpful comments. We also thank two anonymous reviewers whose thoughtful criticisms helped clarify the presentation of our results.

Supporting Information Available: Summary of KIE calculations for the solvolytic transition state, plus the BEBOVIB input (9 pages). See any current masthead page for ordering and Internet access instructions.

JA971316I